8892 *Macromolecules* **2010**, *43*, 8892–8903
DOI: 10.1021/ma101792v

Macromolecules
ARTICLE

Rhodium-Mediated Stereospecific Carbene Polymerization: From Homopolymers to Random and Block Copolymers

Erica Jellema,[†] Anna L. Jongerius,[†] Gert Alberda van Ekenstein,[‡] Steven D. Mookhoek,[§] Theo J. Dingemans,[§] Eva M. Reingruber,[∥,#] Aleksandra Chojnacka,[∥] Peter J. Schoenmakers,[∥] Rik Sprenkels,[⊥] Ernst R. H. van Eck,[⊥] Joost N. H. Reek,[†] and Bas de Bruin*,[†]

[†]*Homogeneous and Supramolecular Catalysis Group, and* [∥]*Polymer-Analysis Group, Van't Hoff Institute for Molecular Sciences, University of Amsterdam, Science Park 904, 1098 XH Amsterdam, The Netherlands,* [‡]*Zernike Institute for Advanced Materials, University of Groningen, Nijenborgh 4, 9747 AG Groningen, The Netherlands,* [§]*Faculty of Aerospace Engineering, Delft University of Technology, Kluyverweg 1, 2629 HS Delft, The Netherlands, and* [⊥]*Institute for Molecules and Materials, Radboud University Nijmegen, Heyendaalseweg 135, 6525 AJ Nijmegen, The Netherlands.* [#]*Current address: Institute of Analytical Chemistry, Johannes Kepler University, 4040 Linz, Austria.*

Received August 5, 2010; Revised Manuscript Received September 14, 2010

ABSTRACT: New stereoregular homo- and copolymers with an ester group at every backbone carbon atom were prepared from ethyl, benzyl and *tert*-butyl diazoacetate (M_w of homopolymers up to 690 kDa and copolymers up to 430 kDa). With polarizing optical microscopy we found that the homopolymers poly(ethyl 2-ylideneacetate) and poly(benzyl 2-ylideneacetate) are able to form stable and accessible thermotropic and lyotropic nematic phases. Both two polymers show relatively high storage moduli up to the glass transition temperature (T_g), as evidenced by dynamic mechanical thermal analysis. The materials retain quite decent storage moduli in a broad elevated temperature range between T_g and T_m. The formation of (block) copolymers was confirmed by a combination of NMR spectroscopy, differential scanning calorimetry and size-exclusion chromatography. 2D-solubility−gradient chromatography−SEC as well as pyrolysis-gas chromatography−mass spectrometry (Py−GC−MS) showed a clear difference in the composition of the random and block copolymers with benzyl and ethyl ester groups. Thermal analysis showed that the homopolymers and block copolymers are semicrystalline, while the random copolymers are completely amorphous. The polymers are thermally stable toward decomposition up to 300 °C (and polymers containing *tert*-butyl ester groups up to 200 °C). The formation of cross-linked polymer was achieved by heating copolymers containing *tert*-butyl ester groups.

Introduction

A long-standing challenge in polymer synthesis is the controlled synthesis of highly stereoregular, high molecular weight carbon-chain polymers with a controllable amount of polar functionalities. Over the past years, several new approaches have been developed to reach this goal. Considerable progress in this field has been achieved with lanthanide metallocene complexes, group 4 early transition metal metallocenes, and alike, which polymerize polar vinyl monomers via coordination−addition polymerization mechanisms (metal-controlled anionic polymerization), allowing the controlled synthesis of both syndiotactic and isotactic (rich) polymers from methylacrylates, acrylates, (meth)acrylamides, acrylonitriles, and vinylketones.[1,2] High triad selectivities can be reached with these methods, but generally low temperatures are required to achieve high stereospecificities. These reactions bear some similarities with anionic polymerization of (meth)acrylates at low temperatures, which also allow a decent stereocontrol.[3] The living character of both anionic and coordination−addition polymerization reactions provides interesting opportunities to prepare block copolymers.

Progress in the development of new late transition metal catalysts for coordination−insertion-type polymerization reactions has made it possible to prepare (random) copolymers of polar vinyl monomers and (aliphatic) alkenes, hence producing interesting new materials with varying microstructures (e.g., side-chain functionalized, main-chain functionalized, random, and block copolymers).[1,4] These catalytic systems produce more than one chain per metal ion (chain transfer), and the most recently developed catalysts even allow a decent control over the amount of the incorporated functionalities. So far there are no reported examples of late transition metal catalysts capable of *stereospecific* polymerization of polar vinyl monomers or *stereospecific* copolymerization of polar vinyl monomers with olefins.[1]

Fascinating new developments in the field of radical-type polymerization reactions show the possibility to gain excellent control over polymer lengths and polydispersities, and modern radical polymerization techniques even make it possible to gain some (albeit still limited) control over the polymer tacticities.[5]

Despite all these intriguing new developments, the problem is by no means solved and many important challenges are still remaining.[1] For example, the synthesis of ***stereoregular*** *carbon-chain polymers which are functionalized at* ***every*** *carbon-atom of the polymer backbone* has proven to be difficult using olefinic monomers, and even the formation of atactic polymers by radical polymerization of 1,2-difunctionalized olefins is nontrivial in some cases.[6] In this respect, C1 polymerization (or "carbene" polymerization) techniques may offer valuable alternative synthetic methods for the synthesis of new materials that are not so

*Corresponding author. Telephone: +31 20 525 6495. Fax: +31 20 525 6422. E-mail: b.debruin@uva.nl.

 Published on Web 10/07/2010

Scheme 1. Rh-Mediated Carbene Polymerization Leading to Fully Functionalized, High Molecular Weight, and Stereoregular (Syndiotactic) Carbon-Chain Polymers

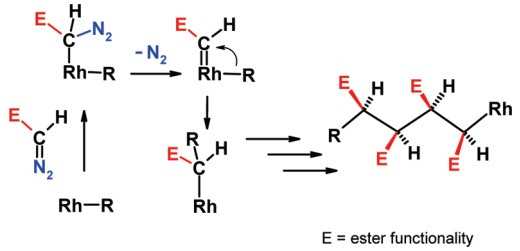

Scheme 2. Synthesis of Catalyst Precursors 1 and 2

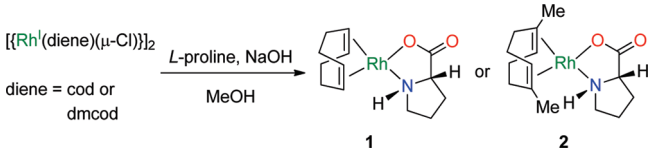

easily accessible by the more common polymerization of C=C double bonds.[7−9] We recently contributed to this field by showing that Rh-mediated carbene polymerization, using diazoesters ($ROC(=O)CH=N_2$) as carbene precursors, allows the preparation of fully functionalized, high molecular weight, and highly syndiotactic carbon-chain polymers,[10−13] in good yields.[13] Presently, this is the only available method to prepare such densely functionalized, sp^3-hybridized[14] polymers in a *stereoregular* manner. The reaction follows a migratory carbene insertion chain propagation mechanism (Scheme 1), and the high syndio-specificity is most likely determined by chain-end control.[11]

With a method in hand to prepare high molecular weight and highly stereoregular fully functionalized polycarbenes, we decided to expand the scope of this new reaction toward the preparation of random and block-type copolymers using three different carbene precursors. The results are described in this paper. Another important goal of this paper is to address the unusual thermal and thermo-mechanical properties of the new highly functionalized, stereoregular polycarbenes. Polar side-chain functionalities of carbon-chain polymers in general have a large and important influence on the polymer material properties (e.g., toughness, paintability/printability, solvent resistance, miscibility).[4a] However, their influence has so far only been investigated for materials in which the mutual influence of the dipole moments of the applied functionalities have a poorly defined (atactic materials)[6,8] and/or diluted effect (C2-polymerization of monofunctionalized olefins in general). In this paper we present for the first time efforts to unravel the influence of multiple dipolar interactions in close proximity along a fully functionalized and stereoregular carbon-chain polymer chain on the material properties of these poly carbenes. As a result we here disclose the unusual material properties of new poly carbene materials, which includes a broad end-use temperature range as well as thermotropic (and lyotropic) liquid crystalline behavior in a broad temperature range (rigid rod behavior).

Results and Discussion

Catalyst Precursors. Previously, we reported different [(diene)Rh^I(*N*,*O*-ligand)] complexes (diene =1,5-cyclooctadiene (cod) (**1** in Scheme 2), *endo*-dicyclopentadiene (dcp), or 2,5-norbornadiene (nbd)) for polymerization of carbenes from ethyl diazoacetate (EDA).[10,11] We showed that the diene ligand plays an important role during the propagation steps, while the *N*,*O*-ligand is likely involved in the initiation

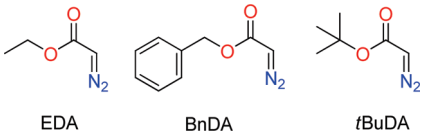

Figure 1. Carbene precursors: ethyl, benzyl, and *tert*-butyl diazoacetate.

of the polymerization. The highest yields were obtained with [(L-prolinate)Rh^I(1,5-cyclooctadiene)] (**1**) (50%)[10,11] and [(L-prolinate)Rh^I(1,5-dimethyl-1,5-cyclooctadiene)] (**2**) (up to 80%) and therefore these catalyst precursors were selected for copolymerization reactions. Complex **2** was stored for several days in air prior to its use in the polymerization reactions in order to obtain higher polymer yields, following the procedures described in one of our previous papers.[13] Complexes **1** and **2** are easily prepared by reacting the corresponding [{Rh^I(diene)(μ-Cl)}]$_2$ (diene =1,5-cyclooctadiene (cod) or 1,5-dimethyl-1,5-cyclooctadiene (dmcod)) with deprotonated L-proline in methanol at room temperature (Scheme 2).

Homopolymerization of Different Diazoesters. We first investigated the behavior of catalyst precursors **1** and **2** in the homopolymerization of different diazoesters. The substrates are ethyl diazoacetate (EDA), a diazoester with an aromatic substituent: benzyl diazoacetate (BnDA) and one with a sterically demanding side group: *tert*-butyl diazoacetate (*t*BuDA) (Figure 1). EDA and *t*BuDA are commercially available and BnDA was prepared by published procedures.[15,16]

The homopolymerization reactions were performed by addition of 50 equiv of diazoester to a solution of catalyst precursor **1** or **2** in chloroform.[10,11] The solution was stirred for 14 h at room temperature. The polymer was obtained by evaporation of the solvent and subsequent precipitation with methanol. After washing with methanol and drying, a white solid was obtained.

Carbenes from EDA and BnDA are polymerized to poly(ethyl 2-ylidene-acetate) (poly(EA)) and poly(benzyl 2-ylidene-acetate) (poly(BnA)), respectively, of high molecular weight (up to 690 kDa) and in moderate to good yields (entries 1, 2, 4, and 5 in Table 1). EDA and BnDA are completely converted into polymers (major fraction), and some dimeric (dialkyl fumarate and maleate) and oligomeric byproducts. The byproducts are soluble in methanol and are separated from the polymer during the precipitation step, as described before.[10−12] Precatalyst **2** gives higher yields than precatalyst **1** for both substrates.

The bulky diazoester *t*BuDA is polymerized to poly(*tert*-butyl 2-ylidene-acetate) (poly(*t*BuA)) in only low yields by both catalyst precursors **1** and **2** (Table 1, entries 3 and 6). The conversion is not complete (65% for **1** and 50% for **2**) and unreacted *t*BuDA was recovered after the reaction. Most of the reacted *t*BuDA was converted into oligomers (~80%, $M_w \sim 1500$ Da, PDI ~ 1.4) and a small amount of dimeric products, di-*tert*-butyl fumarate and maleate (~15%). During the polymerization reaction the polymeric poly(*t*BuA) product precipitates from the reaction mixture in chloroform, which in part explains the low yields (and probably low molecular weights) obtained in these reactions. The isolated white solid is insoluble in most organic solvents, such as chloroform (with and without trifluoroacetic acid), dichloromethane, methanol, toluene, and benzene. Because of its poor solubility, poly(*t*BuA) was analyzed by solid state IR spectroscopy (see Supporting Information).

The solubility behavior of poly(*t*BuA) contrasts markedly with the polymer obtained by radical polymerization of

Table 1. Homopolymerization of EDA, BnDA, and *t*BuDA with 1 and 2[a]

entry	catalyst precursor	diene	substrate	polymer	polymer yield (%)[b]	M_w (kDa)[c]	PDI[c]
1[11]	**1**	cod	EDA	poly(EA)	50	150	3.6
2[13]	**1**	cod	BnDA	poly(BnA)	20	80	6.3
3	**1**	cod	*t*BuA	poly(*t*BuA)	< 5	n.d.	n.d.
4[13]	**2**	dmcod	EDA	poly(EA)	80	670	3.3
5[13]	**2**	dmcod	BnDA	poly(BnA)	50	690	2.7
6	**2**	dmcod	*t*BuA	poly(*t*BuA)	< 5	n.d.	n.d.

[a] Conditions: 0.04 mmol of catalyst precursor, 2 mmol of diazoester, 5 mL of chloroform (solvent), room temperature, reaction time: 14 h. [b] Isolated by precipitation and washing with methanol. [c] SEC analysis calibrated against polystyrene samples in dichloromethane. Poly(*t*BuA) could not be analyzed due to its poor solubility.

Table 2. Copolymerization of EDA, BnDA, and *t*BuDA with Catalyst Precursors 1 and 2[a]

entry	cat.	copolymer	feed ratio (mmol)	M1:M2[b]	polymer yield (%)[c]	M_w (kDa)[d]	PDI[d]
1	**1**	poly(EA-*ran*-BnA)	1:1	1:0.8	30	80	2.8
2	**1**	poly(EA-*ran*-*t*BuA)	1:1	1:0.3	20	100	4.3
3	**1**	poly(BnA-*ran*-*t*BuA)	1:1	1:0.5	5	60	2.4
4	**1**	poly({EA}$_b$-{BnA-*ran*-EA}$_b$)	1.2:2	1:1	30	70	3.6
5	**1**	poly({EA}$_b$-{EA-*ran*-*t*BuA}$_b$)	1.2:2	1:0.2	10	110	4.5
6	**1**	poly({BnA}$_b$-{BnA-*ran*-*t*BuA}$_b$)	1.2:2	1:0.2	5	70	3.8
7	**2**	poly(EA-*ran*-BnA)	1:1	1:0.8	60	430	4.4
8	**2**	poly(EA-*ran*-*t*BuA)	1:1	1:0.3	30	330	3.8
9	**2**	poly(BnA-*ran*-*t*BuA)	1:1	1:0.3	30	100	3.7
10	**2**	poly({EA}$_b$-{BnA-*ran*-EA}$_b$)	1.2:2	1:1.4	45	350	2.4
11[e]	**2**	poly({EA}$_b$-{EA-*ran*-BnA}$_b$)	2:2	1:0.5	30	720	4.2
12	**2**	poly({EA}$_b$-{EA-*ran*-*t*BuA}$_b$)	1.2:2	1:0.2	10	380	4.1
13	**2**	poly({BnA}$_b$-{BnA-*ran*-*t*BuA}$_b$)	1.2:2	1:0.1	20	120	3.9

[a] Conditions: 0.04 mmol of catalyst precursor, 5 mL of chloroform (solvent), room temperature, reaction time = 14 h, random copolymerization: mixture of 2 × 1 mmol of diazoester. Block copolymerization: 1.2 mmol of the first diazoester is added, after 30 min 2 mmol of the second monomer is added. [b] Average composition (estimated by ^{1}H NMR spectroscopy). [c] Isolated by precipitation and washing with MeOH. [d] SEC analysis calibrated against polystyrene samples. [e] Reaction temperature: −20 °C. The second monomer is added after 1 week.

di-*tert*-butyl fumarate, which results in an atactic, but otherwise chemically equivalent polymer.[17] Atactic poly(di-*tert*-butyl fumarate) dissolves in several solvents (benzene, toluene, carbon tetrachloride and tetrahydrofuran). This clearly reveals that the obtained poly(*t*BuA) has very different properties than atactic poly(di-*tert*-butyl fumarate), suggesting that like poly(EA) and poly(BnA), poly(*t*BuA) is also syndiotactic.[11] However, it is not quite clear to us why exactly this leads to a poor solubility in case of poly(*t*BuA).

From these substrate screening experiments, it is clear that EDA and BnDA can be polymerized in reasonable to good yields, leading to high molecular weight polymers. Homopolymerization of *t*BuDA is much less successful. Catalyst precursor **2** performs generally better than catalyst **1**, giving higher yields and longer polymers in case of polymerization of EDA and BnDA. Increasing the steric bulk on going from EDA via BnDA to *t*BuDA leads to lower polymer yields. With catalyst **1**, polymerization of BnDA also leads to shorter polymers than polymerization of EDA, suggesting that the propagation steps in case of BnDA are slower, possibly decreasing the propagation/termination rate ratio, which might thus explain the lower yields. Remarkably, however, this seems not to be the case with catalyst precursor **2**, which gives similar polymer lengths for EDA and BnDA.

Copolymerization of Carbenes from Diazoesters. Having obtained a clear picture of the influence of the substrate substituents and their behavior in the Rh-mediated homopolymerization reactions, we next focused on making copolymers of these substrates. Again catalyst precursors **1** and **2** were used for the copolymerization of carbenes from ethyl (EDA), benzyl (BnDA), and *tert*-butyl (*t*BuDA) diazoacetate (Figure 1). Random copolymerization was performed by adding a mixture of equivalent amounts of monomers A and B to a solution of the catalyst in chloroform, yielding poly(A-*ran*-B). The random copolymers obtained by 1:1 random copolymerization of EDA and BnDA are slightly enriched in the EA component (Table 2, entries 1 and 7). Random copolymers obtained from 1:1 mixtures of EDA and *t*BuDA or BnDA and *t*BuDA are strongly depleted in the *t*BuA component (Table 2, entries 2, 3, 8, and 9). These compositions correlate with the results obtained in the homopolymerization reactions (see above), and thus reflect that EDA is somewhat more reactive in the copolymerization mixtures than BnDA, and *t*BuDA is much less reactive than both EDA or BnDA.

Besides random copolymers, we also attempted to make block copolymers. We previously reported that the Rh-mediated carbene polymerization reactions reveal a linear relation between the polymer yield and M_w, suggesting that the chains terminate slowly and that no significant chain transfer occurs within the time frame of polymerization.[10,11] The polymerization characteristics are such that polymer chain growth is clearly observable within a workable time frame of several hours (Figure S1, Supporting Information). This provides opportunities for one to prepare block copolymers, even though these polymerization reactions are strictly not living.[18] Of course the slow but ongoing termination processes and the fact that the "polymer forming active Rh species" do not survive being completely depleted from the presence of monomer put some limitations to the available time frame and the type of block copolymers that can be prepared with this method. The Rh-mediated carbene polymerization method does, however, allow the synthesis of block copolymers of the type poly{homo M1}−{random M2 > M1}, in which the homoblock M1 is constructed from monomer M1, and where the composition of the random block can be expected being enriched in second monomer M2. This is possible by starting the polymerization with monomer M1, and adding the second monomer M2 after a certain time during which much (but not all) of monomer M1 has been consumed, provided M1 and M2 have similar propagation rates (as is the case for EDA and BnDA).

Scheme 3. Formation of Poly({M1}$_b$−{M2-*ran*-M1}$_b$) Block Copolymers Obtained through Rh-Mediated Carbene Polymerization[a]

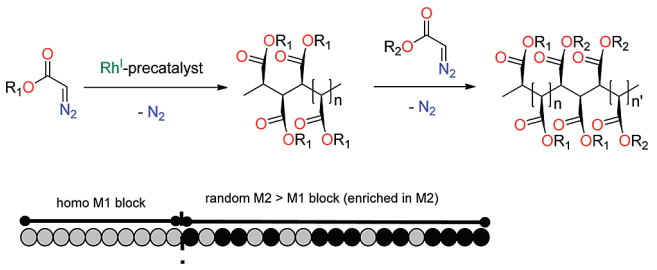

[a]Addition of the second monomer M2 follows 30 minutes after addition of the first monomer M1.

Thus, obtained polymers are different from gradient copolymers produced by so-called forced gradient copolymerization,[19,20] but are likely to reveal quite similar properties. Such copolymers are expected to blend the properties of two different polymers,[19−21] which is potentially useful for the compatibilization of immiscible polymer blends and for the stabilization of emulsions and dispersions.[19] Hence we set-out to prepare densely functionalized, stereoregular, poly{homo M1}−{random M2 > M1} block copolymers through Rh-mediated carbene polymerization reactions.

Block copolymers of the type poly({M1}$_b$−{M2-*ran*-M1}$_b$) were prepared by reacting the catalyst precursor with 1.2 mmol of the first monomer (M1) for 30 min before adding 2 mmol of the second monomer (M2) (Scheme 3). In this way we expected the formation of a polymer with a homoblock of the first monomer M1, followed by a random block M2 > M1 being enriched in the second monomer M2. A similar approach to make block copolymers from the faster propagating monomers EDA/BnDA as the first component and the slower propagating (and faster terminating) *t*BuDA (*vide supra*) as the second component are expected to result in poly{homo M1}−{random M1 > M2} block copolymers. Here the composition of the random block is enriched in the first component (M1 = EA or BnA) despite the larger concentration of the second component M2 = *t*BuDA upon addition. To distinguish between these situations, block polymers of the types poly{homo M1}−{random M2 > M1} and poly{homo M1}−{random M1 > M2} are further denoted as poly({M1}$_b$−{M2-*ran*-M1}$_b$) and poly({M1}$_b$−{M1-*ran*-M2}$_b$), respectively.

With catalyst precursor **2**, homo- and random (co)polymers were obtained in somewhat higher yields than the block copolymers. All obtained polymers show monomodal distributions in their size exclusion chromatograms. At lower temperatures chain termination processes are further suppressed, allowing the formation of longer copolymers, and the second monomer component can be added at a later stage (entry 11, Table 2).

Although carbenes from *t*BuDA are homopolymerized in only low yields (probably due to the steric demand of the *tert*-butyl group), they are incorporated in decent amounts after initiating the reaction with EDA or BnDA. However, propagation from *t*BuDA monomers seems to be slow compared to propagation from EDA, and hence termination occurs before the reaction has completed leading to low overall yields and low *t*Bu−ester incorporation (see, e.g., entries 5 and 12). The incorporation of low amounts of *t*BuA-groups in the formed block after addition of *t*BuDA is due to the reactivity difference between the monomers. The M1 = EA/BnA and M2 = *t*BuA monomers are presumably randomly distributed in this block, but some gradient cannot be excluded in this case.

Overall, Rh^I complex **2** produces the copolymers in higher yields and with higher molecular weights than complex **1**. This was also observed for the homopolymerization reactions (Table 1). Catalyst **2** is also better suited to make block copolymers, leading to longer homoblocks and longer random blocks.

Polymer Analysis

NMR Spectroscopy. ^{13}C NMR spectroscopy shows one relatively sharp signal for the equivalent polymer backbone carbons as well as for the equivalent ester carbonyl carbons for all polymers (see also the Supporting Information for a selection of solid state NMR spectra of the homo- and copolymers). The chemical shifts for the carbonyl (171 ppm) and backbone carbon (45 ppm) atoms are similar to the ones reported for stereoregular poly(ethyl 2-ylideneacetate) reported earlier (see also Table 5).[10,11] Therefore, these polymers must all be highly syndiotactic.[11] Furthermore, ^{1}H NMR spectroscopy confirms the presence of copolymers in the products of the copolymerization reactions. Homopolymers of *t*BuDA can be synthesized in only very low yield and are not soluble in chloroform, while the *tert*-butyl group is clearly observed in the NMR spectra of the copolymers. For the copolymers from EDA and BnDA clearly different chemical shifts are observed than for the homopolymers in the ^{1}H NMR spectra (Table 4). In Figure 2a-d part of the ^{1}H NMR spectra of poly(EA-*ran*-BnA), poly({EA}$_b$−{BnA-*ran*-EA}$_b$) (prepared with **2**) and a mixture of the homopolymers poly(EA) and poly(BnA) are shown. The spectra of the poly({EA}$_b$−{BnA-*ran*-EA}$_b$) block copolymers (Figure 2b and c) reveal the presence of a small amount of homopolymer poly(EA) at δ 4.08 and δ 3.18 ppm, probably formed and terminated in the beginning of the reaction before addition of BnDA.[22]

In principle, these signals could also stem from the poly(EA) homoblock tails which remain uninfluenced by the BnA > EA random block. This seems however unlikely, considering the fact that these signals are actually too small for the sizable EA block formed after 30 min before addition of the second monomer (conversion of EDA with **2** after 30 min: ∼ 80%; poly(EA) M_w ∼ 250 kDa).[23] The peaks of homopolymer poly(EA) are also visible in the ^{13}C NMR spectra of the block copolymer. In Figure 3a−d parts of the ^{13}C NMR spectra of poly(EA-*ran*-BnA), poly({EA}$_b$−{BnA-*ran*-EA}$_b$), and a mixture of the homopolymers poly(EA) and poly(BnA) are shown. The resonances for the copolymers are somewhat broader than for the homopolymers. In the spectra of the poly({EA}$_b$−{BnA-*ran*-EA}$_b$) copolymers, the homopoly(EA) block can be distinguished by the small sharper peak tops at δ 45.3 and 60.7 ppm (Figure 3, parts b and c).

In the ^{1}H NMR spectra, the backbone protons of poly(BnA) (δ 3.6 ppm) resonate at a markedly downfield shifted position compared to the same protons in poly(EA) (δ 3.18 ppm) (Figure 2a), even though the ^{13}C NMR signals of these polymers reveal similar chemical shifts for the backbone and carbonyl carbon atoms (see Table 5). The difference between the signals for the backbone C*H* signals as well as the O−C*H*$_2$ signals for the different homopolymers is almost 0.5 ppm in the ^{1}H NMR spectra. In a random copolymer with ethyl and benzyl ester groups, the backbone C*H* signals of both repeating units shift toward each other (Figure 2d). The backbone protons shift downfield on going from homopoly(EA) via copoly(EA−BnA) to homopoly(BnA), whereas the O−C*H*$_2$−R signals shift upfield with an increasing amount of BnA. The deshielding of the backbone C*H*

Table 3. Thermal Properties of (Co)polymers Determined by Differential Scanning Calorimetry[a]

entry	polymer	M_w (kDa)	PDI	T_g (°C)	T_c (°C)	T_m (°C)	ΔH_m (J/g)
1	poly(EA)	150	3.6	22[b]	80	105	20
2	poly(BnA)	370	2.4	52	154	181	20
3	poly(EA) + poly(BnA)	150; 370	3.6; 2.4	50[c]	84; 161	117; 161	2; 10
4	poly({EA}$_b$-{BnA-*ran*-EA}$_b$)	350	2.4	46	91	120	1
5	poly({EA}$_b$-{EA-*ran*-*t*BuA}$_b$)	380	4.1		89	113	3
6	poly({BnA}$_b$-{BnA-*ran*-*t*BuA}$_b$)	70	3.8	49	163[d]	165[d]	1.5
7	poly(EA-*ran*-BnA)	430	4.4	44			
8	poly(EA-*ran*-*t*BuA)	330	3.8	51			
9	poly(BnA-*ran*-*t*BuA)	100	3.7	62			

[a] General: DSC; heating rate, 1 °C/min. T_m and T_c were determined from the heat flow curves, while T_g was derived from the reversing heat flow curves (1 °C/min). [b] Determined from a cooling scan with 2 °C/min modulated. [c] Only one T_g was observed. [d] Found after partial decomposition of the polymer due to heating to 210 °C.

Table 4. Tabulated ^{1}H NMR Chemical Shift Range (δ in ppm, (Peak Top)) of (Co)polymers of EDA, BnDA, and *t*BuDA with Numbering Scheme

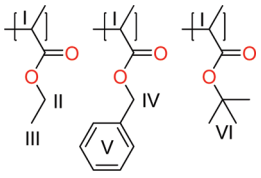

		proton					
polymer	freq (MHz)	I	II	III	IV	V	VI
poly(EA)[10]	500	3.1−3.3 (3.2)	4.0−4.2 (4.1)	1.1−1.3 (1.2)			
poly(BnA)[13]	500	3.5−3.7 (3.6)			4.5−5.0 (4.7)	7.0−7.3 (7.1)	
poly(EA-*ran*-BnA)	500	3.2−3.7 (3.4)	3.7−4.2 (3.9)	0.8−1.4 (1.1)	4.6−5.2 (4.9)	7.0−7.6 (7.2)	
poly(EA-*ran*-*t*BuA)	400	3.0−3.3 (3.2)	3.9−4.2 (4.1)	1.1−1.3 (1.2)			1.3−1.6 (1.4)
poly(BnA-*ran*-*t*BuA)	400	3.3−3.8 (3.6)			4.5−5.2 (4.8)	6.9−7.5 (7.1)	1.0−1.5 (1.2)
poly({EA}$_b$-{BnA-*ran*-EA}$_b$)[a]	500	3.1−3.2 (3.2), 3.2−3.7 (3.5)	3.6−4.0 (3.8), 4.0−4.1 (4.1)	0.8−1.1 (0.9), 1.1−1.3 (1.2)	4.6−5.1 (4.8)	6.9−7.4 (7.1)	
poly({EA}$_b$-{EA-*ran*-*t*BuA}$_b$)	500	3.1−3.2 (3.2)	3.9−4.2 (4.1)	1.1−1.3 (1.2)			1.3−1.6 (1.4)
poly({BnA}$_b$-{BnA-*ran*-*t*BuA}$_b$)	400	3.5−3.7 (3.6)			4.5−5.0 (4.7)	6.9−7.5 (7.1)	1.0−1.6 (1.2, 1.3)

[a] Mixture of poly(EA) and poly({EA}$_b$-{BnA-*ran*-EA}$_b$).

Table 5. Tabulated ^{13}C NMR Chemical Shift Values (δ in ppm) of (Co)polymers of EDA, BnDA, and *t*BuDA with Numbering Scheme

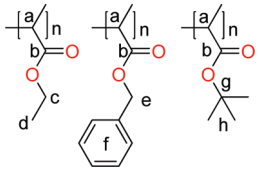

		carbon atom							
polymer	freq (MHz)	a	b	c	d	e	f	g	h
poly(EA)[10]	125	45	171	61	14				
poly(BnA)[13]	125	45	171			67	135, 128, 127		
poly(EA-*ran*-BnA)	125	45	171	61	14	67	136, 128, 127		
poly(EA-*ran*-*t*BuA)	100	45	171	60	14			81	28
poly(BnA-*ran*-*t*BuA)	100	[a]	171			67	136, 128, 127	[a]	28
poly({EA}$_b$-{BnA-*ran*-EA}$_b$)[b]	125	45	171	61	14	67	136, 128, 127		
poly({EA}$_b$-{EA-*ran*-*t*BuA}$_b$)	125	45	171	61	14			81	28
poly({BnA}$_b$-{BnA-*ran*-*t*BuA}$_b$)	100	[a]	171				136, 128, 127	[a]	28

[a] Resonance not observed. [b] Mixture of poly(EA) and poly({EA}$_b$−{BnA-*ran*-EA}$_b$).

and shielding of the −O−CH_2−R protons can be explained by inter- or intrachain interactions of the aromatic rings of the benzyl groups involving $\pi-\pi$ stacking of the aromatic rings (Figure 4).

The effects are maximized in homopolymers of BnDA, and smaller in the copolymers. In poly({EA}$_b$−{BnA-*ran*-EA}$_b$) (Figure 2, middle) the first part of the polymer consists only of poly(EA) and the last part of the polymer consists mainly of poly(BnA). Therefore, the effect of the $\pi-\pi$ stacking on the −O−CH_2−Ph ^{1}H NMR chemical shifts is smaller than in the random copolymer. Remarkably, all −O−CH_2−Me functionalities in the copolymers are upfield shifted, to roughly the same extent for the random and the poly({EA}$_b$−{BnA-*ran*-EA}$_b$) copolymers. These data thus do not allow the direct detection of the presence of an EA-homo block with ^{1}H NMR spectroscopy, while such blocks (with a sizable length: $M_w \sim 250$ kDa for **2**) must be present considering the way the polymers were prepared. Since no (large amount of) pure homopoly(EA) is obtained either, the EA moieties of the poly(EA)-homoblock tails in the

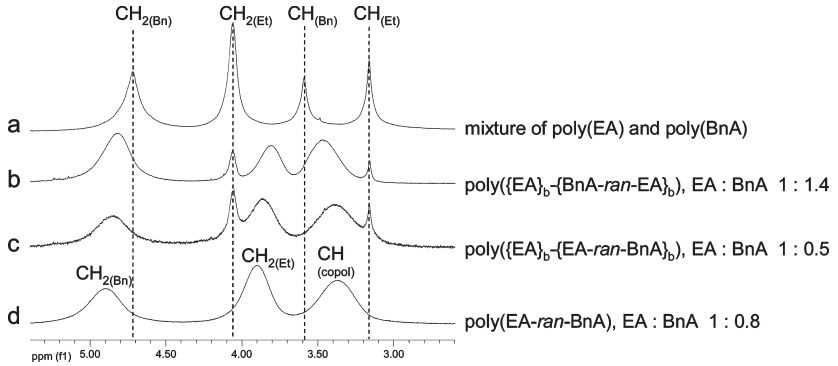

Figure 2. Part of the ^{1}H NMR spectra (500 MHz, $CDCl_3$, 298 K) of homo and copolymers of EDA and BnDA. Key: poly(EA), entry 4, Table 1; poly(BnA), entry 5, Table 1; poly(EA-*ran*-BnA), entry 7, Table 2; poly({EA}$_b$−{BnA-*ran*-EA}$_b$), entries 10 and 11, Table 2.

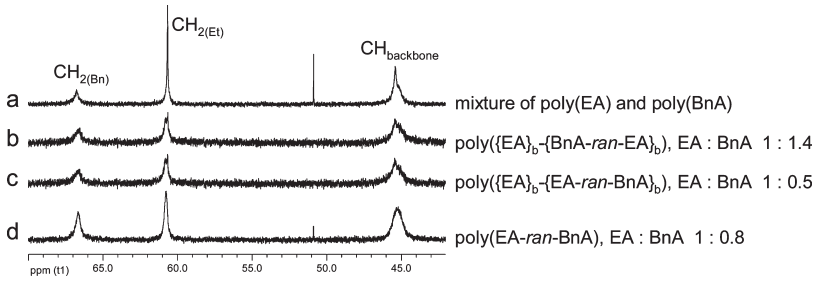

Figure 3. Part of the ^{13}C NMR spectra (125 MHz, $CDCl_3$, 298 K) of homo and copolymers of EDA and BnDA. Key: poly(EA), entry 4, Table 1; poly(BnA), entry 5, Table 1; poly(EA-*ran*-BnA), entry 7, Table 2; poly({EA}$_b$−{BnA-*ran*-EA}$_b$), entries 10 and 11, Table 2.

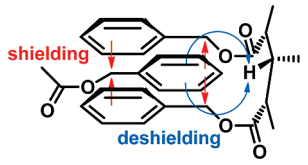

Figure 4. Schematic representation of chain interactions.

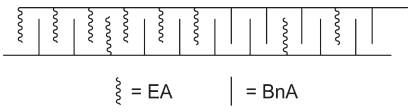

Figure 5. Schematic representation of the intercalation of the polymer chain(s).

poly({EA}$_b$−{BnA-*ran*-EA}$_b$) polymer apparently resonate at the same frequency as the randomly distributed EA moieties in the random polymer, while the EA moieties of both these copolymers resonate at a clearly different position than those in poly(EA) homopolymer. To explain these observations we propose an (on average) intercalation of the poly(EA) homoblock tails with the BnA moieties of the {BnA-*ran*-EA} random blocks (which are strongly enriched in BnA) of these polymers (Figure 4), thus explaining the observed upfield shifts of the homo-EA block signals in the poly({EA}$_b$−{BnA-*ran*-EA}$_b$) block polymers. Hence, on average all EA moieties of these block copolymer are influenced by these interactions (for a schematic representation, see Figure 5).

Chromatographic Analysis

LC × SEC. The following polymers were examined with online coupled gradient-elution liquid chromatography (LC) and SEC: poly(EA) (M_w = 150 kDa, PDI = 3.6, entry 1, Table 1), poly(BnA) (M_w = 370 kDa, PDI = 2.4), poly(EA-*ran*-BnA) (M_w = 80 kDa, PDI = 2.8, EA:BnA = 1:0.8, entry 1, Table 2) and poly({EA}$_b$−{BnA-*ran*-EA}$_b$) (M_w = 70 kDa, PDI = 3.6, EA:BnA = 1:1, entry 4, Table 2).[24] In gradient-elution LC, the retention is mainly a function of chemical composition but is also affected by the sequence distribution and by the molecular weight.[25]

Poly(EA) is less retained than poly(BnA). The two copolymers elute − as expected − between the two homopolymers, poly({EA}$_b$−{BnA-*ran*-EA}$_b$) somewhat later than poly(EA-*ran*-BnA). For a high-molecular-weight random copolymer retention is directly related to the chemical composition.[26] If sufficiently long random blocks are enriched enough in one of two components, the retention is shifted toward the elution time of the corresponding homopolymer.[27] The difference in retention time for poly({EA}$_b$−{BnA-*ran*-EA}$_b$) and poly(EA-*ran*-BnA) is thus indicative for the different sequence distribution and higher BnA content in poly({EA}$_b$−{BnA-*ran*-EA}$_b$).

Every gradient-elution chromatogram is − to a certain extent − also convoluted by an effect of molecular weight, with the smallest molecules eluting first (i.e., opposite to what is observed in SEC).[25] Therefore, combining gradient-elution LC and SEC enables the separation of substances, which would coelute in one-dimensional SEC and gradient-elution LC respectively.

In a comprehensive two-dimensional combination of gradient-elution LC and SEC (LC × SEC) every fraction eluting from the first dimension (LC) column is cross-fractionated on a second (SEC) column.[28] The result is a two-dimensional chromatogram as illustrated in Figure 6. The gradient-elution LC × SEC chromatogram reveals that in the high-molecular-weight-region poly({EA}$_b$−{BnA-*ran*-EA}$_b$) (Figure 6c) is largely enriched in BnA monomer. A small amount of homopoly(EA) material is also present. This is in line with the results of ^{1}H NMR spectroscopy. Homopoly(BnA) material is not found.

Py−GC−MS. Poly(EA), poly(BnA), poly(EA-*ran*-BnA), and poly({EA}$_b$−{BnA-*ran*-EA}$_b$) were also characterized

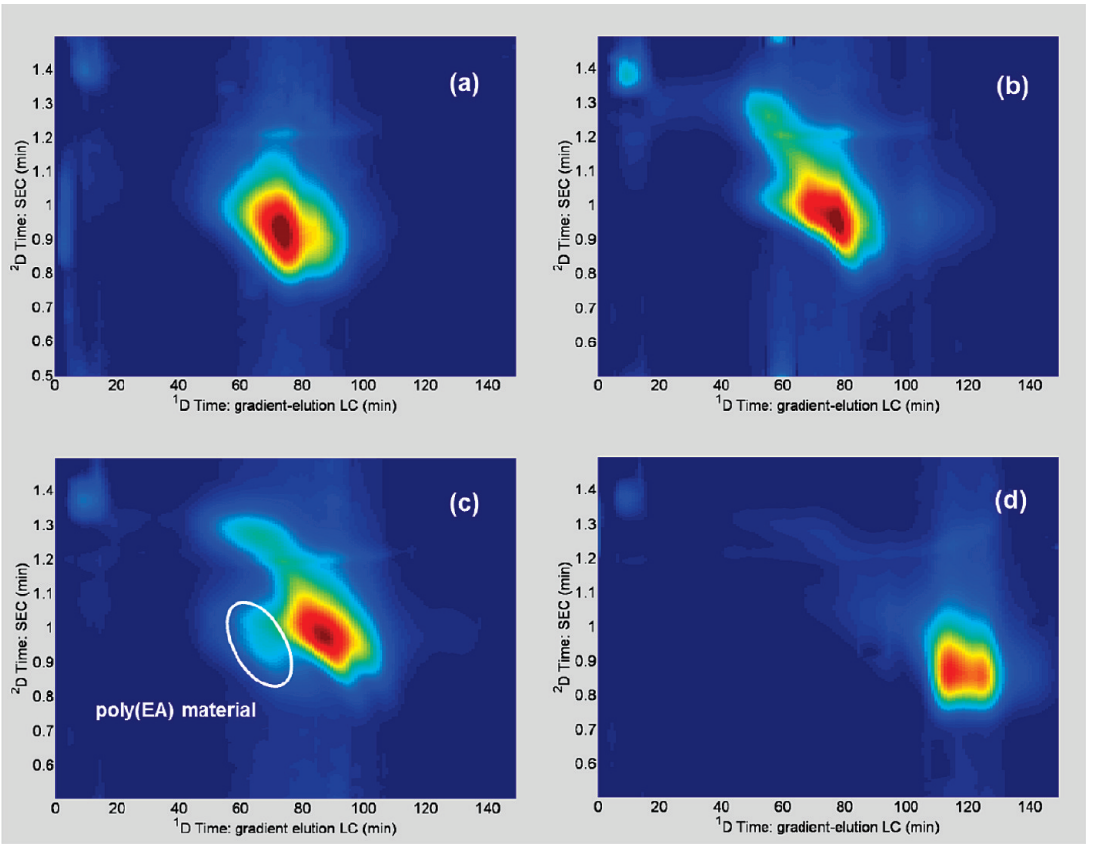

Figure 6. Comprehensive gradient-elution LC × SEC chromatograms: (a) poly(EA) (entry 1, Table 1); (b) poly(EA-*ran*-BnA) (entry 1, Table 2); (c) poly({EA}$_b$−{BnA-*ran*-EA}$_b$) (entry 4, Table 2); (d) poly(BnA) (M_w = 370 kDa, PDI = 2.4).

with pyrolysis−gas chromatography−mass spectrometry (Py−GC−MS) (Figure 7), which provided more insight in the sequence distribution of these different polymers. During pyrolysis, polymers are decomposed into smaller fragments, which are separated and detected with GC−MS.

For poly(EA) only a single peak is observed, which corresponds to the EA dimer (Figure 7a). The pyrolysis of poly(BnA) results in four peaks: the first three are smaller fragments of the polymer, while the last one corresponds to the BnA dimer (Figure 7b). In the pyrogram of the copolymers an additional peak was observed (Figure 7, parts c and d). From the MS spectrum this peak was tentatively identified as EA−BnA dimer, which is characteristic for the random-copolymeric material. The presence of homopolymeric EA blocks and random BnA-EA blocks which are strongly enriched in the BnA component, within the poly({EA}$_b$−{BnA-*ran*-EA}$_b$) block copolymer already observed in ^{1}H NMR and in gradient-elution LC × SEC is supported by the observation of quite intense peaks of the EA dimer and BnA dimer fragments and the substantially reduced intensity of the mixed EA−BnA dimer fragments (compared to the signals in the chromatogram of poly(EA-*ran*-BnA) of roughly the same average composition, as shown in Figure 7c). These data, in combination with the information obtained from the 2D LC × SEC and NMR measurements, clearly illustrate the differences between the poly({EA}$_b$−{BnA-*ran*-EA}$_b$) block copolymer and the random poly(EA-*ran*-BnA) copolymer.

Thermal Analysis

In 2006, we suggested the possible thermotropic liquid crystallinity of poly(EA).[10] We observed birefringence for this polymer and we tentatively assigned the transition observed in the differential scanning calorimetry thermogram upon heating as a transition from the crystalline to a liquid crystalline phase. Here, we report new insights in these phase transitions for the homopolymers poly(EA) and poly(BnA).

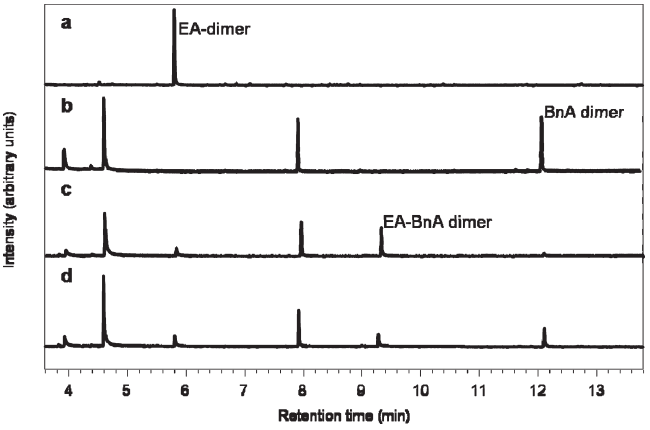

Figure 7. Py−GC−MS chromatograms: (a) poly(EA) (Table 1, entry 1); (b) poly(BnA) (M_w = 370 kDa, PDI = 2.4); (c) poly(EA-*ran*-BnA) (entry 1, Table 2); (d) poly({EA}$_b$−{BnA-*ran*-EA}$_b$) (entry 4, Table 2).

Polarizing Optical Microscopy. Carbon chain polymers, which are sp^3-based, such as polyolefins or polycarbenes, are typically thought of as highly flexible polymers which display either amorphous or semicrystalline morphologies. Although seldomly observed in all sp^3-based backbone polymers, the possibility of liquid crystalline (LC) phases in both poly(EA) and poly(BnA) should be considered. The high degree of substitution would impede the free rotation around the flexible C−C backbone linkages, hindered by the dipolar interactions of the ester moieties in close proximity, thus resulting in a stiff

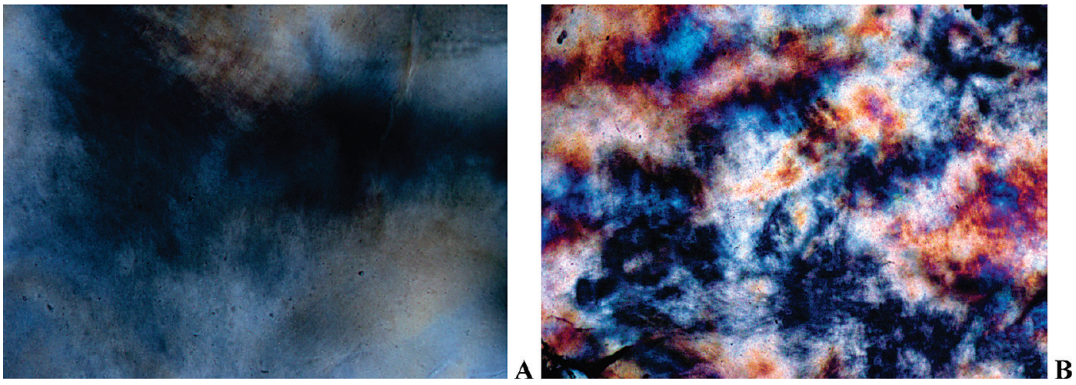

Figure 8. (a) Lyotropic nematic phase of poly(EA) at 25 °C (20 wt % in CH_2Cl_2) with crossed polarizers, magnification 20×. (b) Thermotropic nematic melt of poly(EA) at 230 °C with crossed polarizers, magnification 20×.

helical rod-type molecule. To date, very few examples have been reported where LC properties where observed in polyolefin-alike carbon-chain polymers. Ungar[29] reported the presence of a hexagonal mesophase in polyethylene at 280−307 °C and 8 kbar external pressure, whereas de Jeu et al.[30,31] reported on the shear-induced smectic ordering in isotactic polypropylene. In both cases liquid crystallinity could only be observed under rather extreme conditions, at high temperatures and high pressures, or upon applying large shear forces. More recently Naga et al. demonstrated liquid crystalline behavior in poly(methylene-1,3-cyclopentane), a polyolefin synthesized from rigid 1,3-cyclopentane units.[32] This polymer showed a nematic mesophase at ambient conditions (25 °C, 1 bar).

The phase behavior of poly(EA) and poly(BnA), both in solution and in the melt, was investigated using polarizing optical microscopy. Since both polymers are soluble in CH_2Cl_2 we prepared 20 wt % solutions and found that both polymers form nematic lyotropic phases at room temperature. In this LC phase, the polymer rods display long-range order but lack positional order. The nematic phases could be oriented using shear and upon slow evaporation of the solvent the nematic textures were preserved. The melt behavior of both polymers was investigated using an optical microscope equipped with a hot-stage. Samples were heated under ambient conditions using a heating rate of 10 °C/min and we found that both polymers form highly viscous nematic melts. Because of the high molecular weight of the polymers the nematic melts were difficult to align using shear. Both polymers show excellent thermal stabilities and broad nematic ranges, i.e. the nematic-to-isotropic coincides with the onset of thermal decomposition, which becomes apparent above 300 °C. Both polymers show a remarkably stable nematic window of ∼190 °C for poly(EA) and ∼140 °C for poly(BnA). The lyotropic and thermotropic textures of poly(EA) are shown in Figure 8. Poly(BnA) shows similar textures. The ability to access highly aligned fibers and films from sp^3-based (i.e., polycarbene or polyolefin based) LC materials will enable a whole new class of structural and functional applications previously not accessible. We are currently exploring the rheological behavior and XRD patterns of the LCs, both in solution and in the melt.

Dynamic Mechanical Thermal Analysis (DMTA). The thermo mechanical properties, i.e. the storage modulus (E') and loss modulus (E''), were measured for poly(EA) and poly(BnA) between −100 and 175 °C and the results are given in Figure 9. For reasons of clarity only the data at 1 Hz are displayed in the Figure, which is representative for the rest of the data, as the general trend of the polymers did not change much with frequency. Both polymers showed relatively high storage moduli up to the glass-transition temperature T_g (for both polymers above room temperature); ∼3.5 GPa. The recorded T_g values at 1 Hz are in good agreement with the values found in the DSC measurements (Table 3). Here a T_g of 31 and 57 °C, as determined at maximum E'', are found for poly(EA) and poly(BnA) respectively.

The high plateau modulus above the T_g (∼0.5−1.0 GPa) indicates that both polymers exhibit some degree of crystallinity. This semicrystalline morphology is rather useful since it expands the practical end-use temperature of both polymers far beyond the T_g. The materials retain quite decent storage moduli in a broad elevated temperature range between T_g and T_m. At the end of the rubber plateau the temperature approaches the melting point (T_m) and the material starts to flow under the applied load in the nematic melt, indicated by another drop of the storage modulus and an increase in tan δ. The temperature at which this occurs, differs substantially for both materials: a flow point of 112 °C was found for poly(EA) and 158 °C for poly(BnA).

Differential Scanning Calorimetry. Results of differential scanning calorimetric (DSC) measurements of all homo- and copolymers are shown in Table 3. The homo- and poly($\{M1\}_b$-$\{M2$-*ran*-$M1\}_b$) block copolymers are semicrystalline (showing both T_g and T_c and T_m), while the random copolymers are completely amorphous (showing only T_g). These data provide additional evidence for the different structure of the random and block copolymers. The observed transitions for the copolymers with benzyl and ethyl ester groups were found at temperatures between the transitions of poly(EA) and poly(BnA). A mixture of poly(EA) and poly(BnA) showed transitions at similar temperatures as the homopolymers (entry 3). However, for this mixture, only one glass transition was found.

Samples of copolymers containing *t*BuA groups were heated to 180 °C in the first cycle(s) to prevent decomposition by isobutene loss (*vide infra*). However, for poly($\{EA\}_b$−$\{BnA$-*ran*-*t*$BuA\}_b$) no crystallization or melting transitions were found. After heating to 210 °C, T_c and T_m transitions were observed (entry 6), but presumably the polymer partially decomposed at these elevated temperatures.

Thermogravimetric Analysis. All (co)polymers were subjected to thermogravimetric analysis. The thermal properties of poly(EA) have been reported previously,[10] but are included here for comparison. Polymers containing ethyl and/or benzyl ester moieties decompose above 300 °C. For these copolymers no stabilizing or destabilizing effects were observed; the degradation curves of the copolymers lie between those of the corresponding homopolymers (Figure 10a).

The atactic analogue of poly(EA), prepared from EDA with Pd-based catalysts by Ihara et al., showed a much lower decomposition temperature: at 183 °C, 10% of the atactic polymer is decomposed.[33]

The decomposition of poly(*t*BuA) differs from the decomposition of poly(di-*tert*-butyl fumarate) reported in the literature.[34] Poly(di-*tert*-butyl fumarate) starts to decompose around 200 °C and forms poly(fumaric acid) in one step. However, poly(*t*BuA) arrives to approximately 50% weight decrease (corresponding roughly to quantitative loss of isobutene) in two steps (Figure 10b). It is not clear whether this behavior is caused by higher tacticity of poly(*t*BuA) compared to poly(di-*tert*-butyl fumarate). The subsequent smoother step to 43% of the weight could be due to anhydride formation (*vide infra*).

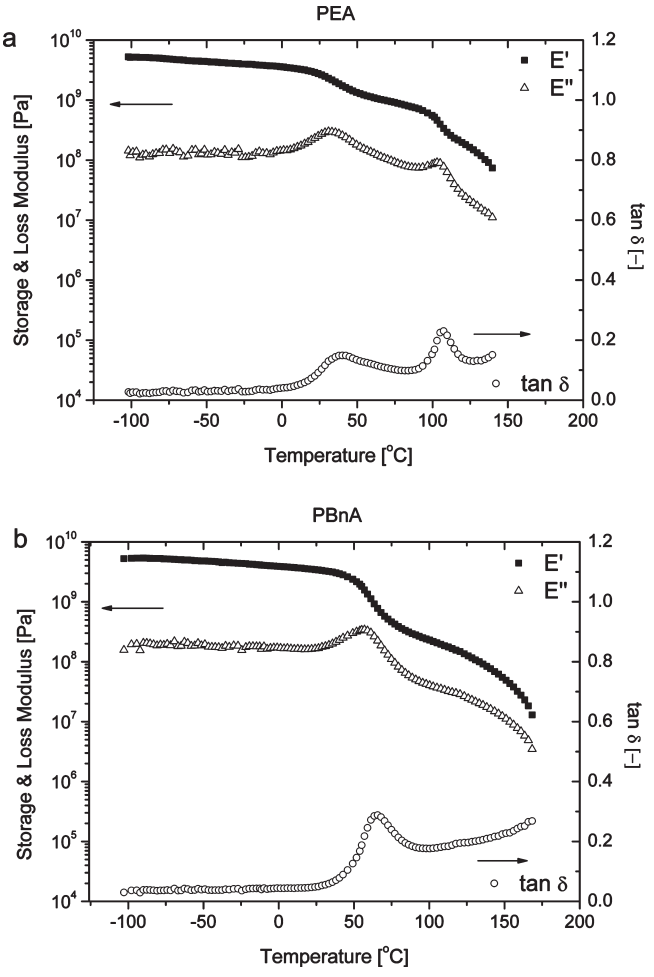

Figure 9. (a) Storage (E') and loss modulus (E'') between −100 and 175 °C for poly(EA) and (b) poly(BnA) at 1 Hz. Experiments were performed under nitrogen at a heating rate of 2.5 °C/min.

The degradation curve of poly({EA}$_b$−{EA-*ran*-*t*BuA}$_b$) (entry 12, Table 2) also clearly shows stepwise degradation, starting at 240 °C (Figure 10b). The weight loss in the first step corresponds with loss of isobutene from the *tert*-butyl groups, which was expected to result in formation of carboxylic acid groups. Since this is potentially interesting for the formation of amphiphilic polymers, the thermolysis was carried out on a preparative scale (*vide infra*).

Thermolysis of *t*Bu Ester Containing Copolymers. The white solid polymeric materials were subjected to thermal degradation under continuous evacuation at 180 °C for several hours. After heating, the polymer does not dissolve in either polar or apolar solvents, whereas all discussed (co)polymers with intact ester groups are soluble in e.g. chloroform or dichloromethane. Therefore, the product was analyzed by solid state NMR spectroscopy (Figure 11).

Before heating, all the expected signals of the copolymers are visible. After heating, the signal for the *tert*-butyl CH_3 groups has decreased in intensity and the quaternary carbon signal has almost disappeared. If carboxylic acid groups are formed, the corresponding carbonyl signal should be observed more downfield around 180 ppm.[35] The spectra do not reveal such signals. Formation of anhydrides by loss of isobutene and subsequent reaction of the carboxylic acid with neighboring ester moieties (with loss of alcohol) seems the most likely explanation (Scheme 4). This was confirmed by IR spectroscopy (*vide infra*). Formation of a small amount of anhydrides was also observed when solid poly(di-*tert*-butyl fumarate) was thermally degraded.[17]

The thermal decomposition of solid poly(EA-*ran*-*t*BuA) and poly({EA}$_b$−{EA-*ran*-*t*BuA}$_b$) was monitored in time by IR spectroscopy (Figure 12). For both materials the appearance of two additional signals is observed at ∼1780 and ∼1855 cm^{-1}, corresponding to the formation of anhydrides.[36] For poly(EA-*ran*-*t*BuA) (Figure 12a) the anhydride signals are stronger, which can be explained by the higher *tert*-butyl ester content. Note that quantitative loss of one isobutene and one *t*BuOH moiety per two monomer units from the polymer corresponds to a weight loss of 57%, in qualitative agreement with the thermo-gravimetric analytical data (∼50% weight loss observed at ∼300 °C).

The low solubility of the thermally degraded *t*BuA-containing polymers most likely indicates the formation of anhydride cross-links between polymer chains. In this way

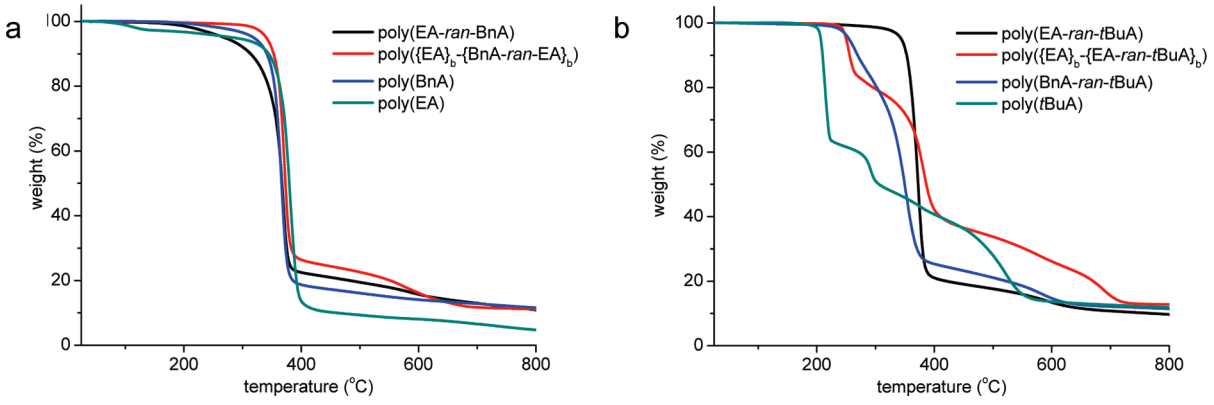

Figure 10. Weight loss curves of (a) homo- and copolymers of carbenes from ethyl and benzyl diazoacetate and (b) copolymers of carbenes from *tert*-butyl diazoacetate.

simple heating of the polymers containing *tert*-butyl ester groups induces the formation of new, highly functionalized cross-linked polymers. This could be interesting from the perspective of applications as thermo-hardening polymers in, e.g., glues or paints. Furthermore, the presence of a reactive anhydride moiety opens up the possibility for post-modification of the material by for example re-esterification by reaction with alcohols.[36]

Conclusions

In conclusion, polymerization of carbenes from diazoesters by Rh^I precatalysts provides a method to obtain high molecular weight and stereoregular (co)polymers with a polar side group at every backbone carbon atom. The homopolymers from ethyl and benzyl diazoacetate were analyzed by polarizing optical microscopy and revealed thermotropic and lyotric liquid crystallinity (nematic phases), which is remarkable for sp^3-based carbon chain polymers. Furthermore, these homopolymers have relatively high storage moduli up to T_g and above.

The formation of random and poly($\{M1\}_b$–$\{M2$-*ran*-$M1\}_b$) block copolymers of carbenes from different diazoesters was confirmed by NMR spectroscopy, differential scanning calorimetry and size-exclusion chromatography. Both with 2D–solubility-gradient chromatography–SEC and Py–GC–MS, a clear difference was observed between random poly(EA-*ran*-BnA) and block-type poly($\{EA\}_b$–$\{$BnA-*ran*-$EA\}_b$) copolymers prepared from ethyl diazoacetate and benzyl diazoacetate, with the random block of the homorandom block polymer being strongly enriched in the BnA component. In particular, Py–GC–MS showed that the polymerization of carbenes from diazoesters is a suitable method to synthesize poly($\{EA\}_b$–$\{$BnA-*ran*-$EA\}_b$) block copolymers. Copolymers containing *tert*-butyl ester groups could be converted into cross-linked polymers by simple heating.

The semicrystalline behavior of the homopolymers and the poly($\{M1\}_b$–$\{M2$-*ran*-$M1\}_b$) block copolymers and amorphous behavior of the random copolymers was revealed by thermal analysis. This behavior is likely due to rigid-rod behavior of the polymer chain, induced by the enforced dipolar interactions between the densely packed carbonyl moieties of the polymers. The implications of these studies for the mechanism of the reaction, the optimization of the reaction conditions and the applications of these new materials are currently under investigation.

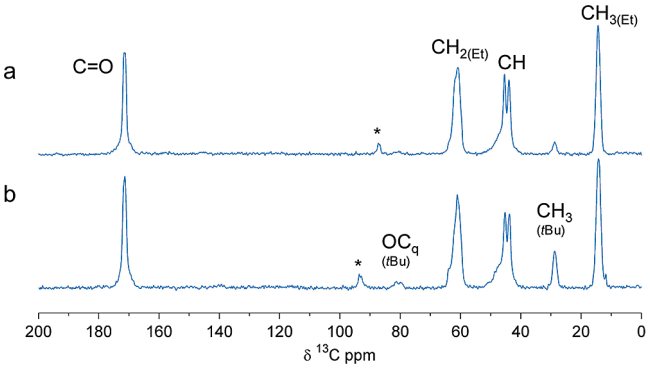

Figure 11. ^{13}C CPMAS NMR spectra of poly($\{EA\}_b$–$\{EA$-*ran*-*t*BuA$\}_b$) before (b) and after heating (a) at 180 °C under vacuum for 6 h. Assignments are indicated in the figure, spinning sidebands are marked with an asterisk.

Scheme 4. Formation of Intra- and Intermolecular Anhydrides from Poly(*t*BuA)

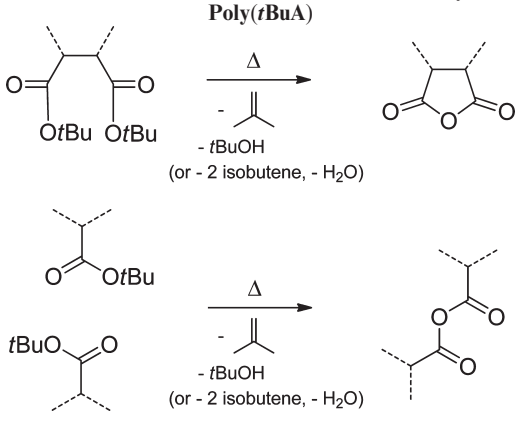

Experimental Section

General Procedures. All manipulations, except the work-up of polymerization reactions, were performed under an argon atmosphere using standard Schlenk techniques. Methanol and dichloromethane distilled from calcium hydride under nitrogen were used for metal complex synthesis. The syntheses and catalytic activities of [(L-prolinate)Rh^I(1,5-cyclooctadiene)] (**1**) and [(L-prolinate)Rh^I(1,5-dimethyl-1,5-cyclooctadiene)] (**2**) have been reported previously.[10,11,13] Complex **2** was stored in air prior to the polymerization reactions.[13] Benzyl diazoacetate[16] (BnDA) was synthesized from glycine benzyl ester hydrochloride[15] according to literature procedures. All other chemicals were purchased from commercial suppliers and used without further purification. Solution state NMR spectroscopy experiments were carried out on a Varian Inova 500 spectrometer (500 and 125 MHz for ^1H and ^{13}C, respectively), a Bruker

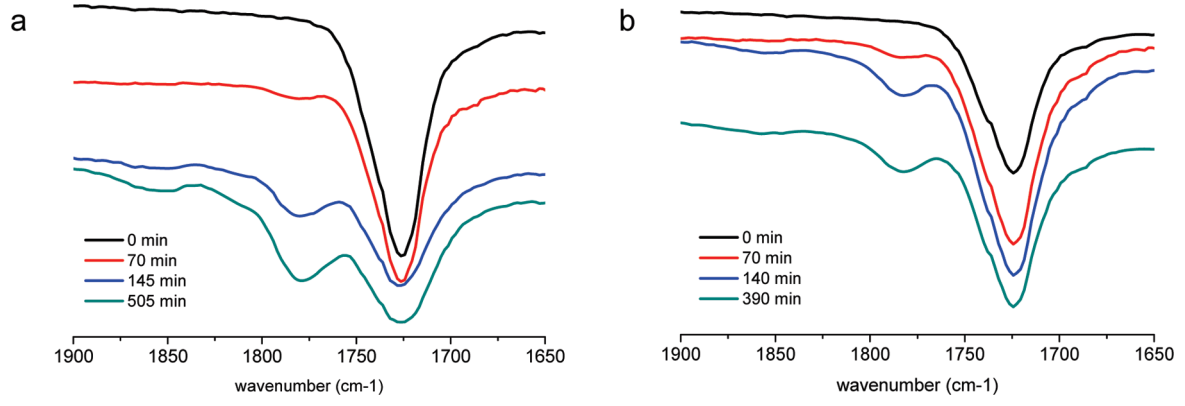

Figure 12. IR spectra of thermolysis of *t*Bu-ester containing copolymers: (a) poly(EA-*ran*-*t*BuA) (entry 2 in Table 2) and (b) poly($\{EA\}_b$–$\{EA$-*ran*-*t*BuA$\}_b$) (entry 5 in Table 2).

ARX 400 spectrometer (400 and 100 MHz for ^{1}H and ^{13}C, respectively) or a Varian Mercury 300 spectrometer (300 and 75 MHz for ^{1}H and ^{13}C, respectively). Solvent shift reference for ^{1}H NMR spectroscopy: $CDCl_3$, δ_H = 7.26 ppm. For ^{13}C NMR spectroscopy: $CDCl_3$, δ_C = 77.0 ppm. Solid State NMR ^{13}C CP MAS NMR spectra were measured on a Chemagnetics 300 MHz spectrometer with a Bruker 2.5 mm MAS probe tuned to a resonance frequency for ^{13}C of 75.480 and 300.149 MHz for ^{1}H. Magic angle spinning was between 5.3 and 6.4 kHz while the number of acquisitions ranged from 3750 to 8192. Protons were decoupled during 30 ms of acquisition with an rf-field strength of 120 kHz and a CM decoupling sequence which was optimized on glycine (8.4 μs pulses and 3° modulation amplitude). Cross-polarization was performed with a 1 ms contact time with an rf field of 71 kHz and a 2% ramp for ^{1}H and 66 kHz for ^{13}C. Chemical shifts were referenced externally using the CH_2 resonance of solid adamantane (δ = 38.48 ppm). IR solid state measurements were performed on a Shimadzu FTIR 8400S spectrometer equipped with a Specac MKII Golden Gate single reflection ATR system. Molecular weight distributions were measured using size-exclusion chromatography (SEC) on a Shimadzu LC-20AD system with two PLgel 5 μm MIXED-C (300 mm × 7.5 mm) columns (Polymer Laboratories) in series and a Shimadzu RID-10A refractive-index detector, using dichloromethane as mobile phase at 1 mL/min and T = 35 °C. Polystyrene standards in the range of 760−1 880 000 g/mol (Aldrich) were used for calibration. Thermo gravimetric experiments were executed with a Perkin-Elmer TGA7 with a heating rate of 10 °C/min under a nitrogen atmosphere. Differential scanning calorimetry was performed using a DSC Q1000 (TA-Instruments) in the modulated mode. The heating rate was 1 °C/min, the amplitude of temperature modulation was 0.5 °C and the period of modulation 60 s. Melting temperatures T_m and crystallization temperatures T_c were determined from the heat flow curves, while glass transition temperatures T_g were derived from the reversing heat flow curves. For the determination of T_g of poly(EA) a cooling rate of 2 °C/min modulated was used.

All Py−GC−MS analyses were performed on a Shimadzu GCMS-QP2010plus instrument equipped with an Optic 3 PTV injector from ATAS GL. GC analysis was carried out on a 15 m × 0.25 mm i.d. TC 5MS (5% phenyl−methylpolysiloxane) column with a film thickness of 0.25 μm (GL Sciences) using helium as a carrier gas at a flow rate of 1.6 mL/min. All samples were dissolved in chloroform at approximately the same concentration (30 μg/mL). A 1 μL sample of the solution was injected into the PTV injector. The PTV was programmed from 40 to 100 °C at 5 °C/s and after elimination of the solvent at 30 °C/s up to 550 °C (temperature was optimized for all analyzed polymers). The GC temperature program started once the PTV injector had reached the final pyrolysis temperature. The GC temperature program run from 45 to 320 °C at 20 °C/min. The initial and final holding periods were 3 min each. The mass spectrometer was used in the full-scan mode. Electron ionization mass spectra at 70 eV electron energy were obtained across the range of 50−500 Da.

Polymerization of Carbenes from Diazoesters. The different polymerization reactions were carried out as described below. The work-up procedure is the same for each reaction.

Homopolymerization. Alkyl diazoacetate (2 mmol) was added to a yellow solution of catalyst (0.04 mmol) in chloroform (5 mL).

Random Copolymerization. A mixture of two alkyl diazoacetates (2 × 1 mmol) was added to a yellow solution of catalyst (0.04 mmol) in chloroform (5 mL).

Block Copolymerization. The first alkyl diazoacetate (1.2 mmol) was added to a yellow solution of catalyst (0.04 mmol) in chloroform (5 mL). The mixture was stirred for 30 min at room temperature, before the second alkyl diazoacetate (2 mmol) was added. (The conversion of EDA and the M_w of the formed poly(EA) after 30 min was determined with ^{1}H NMR spectroscopy and SEC, respectively.)

Polymerization Workup. The mixture was stirred for 14 h at room temperature. Subsequently the solvent was removed *in vacuo* and methanol was added to the oily residue. The precipitate was centrifuged and washed with methanol until the washings were colorless. The resulting white powder was dried *in vacuo*.

Thermolysis of *t*Bu Ester Containing Copolymers. A sample of the copolymer was heated to 180 °C under continuous vacuum for several hours. The color of the solid changed from white to slightly brown during the first hour and remained the same during the experiment. The progress of the thermolysis was monitored with solid state IR spectroscopy.

Polymer NMR Spectroscopy. All polymers were dissolved in deuterated chloroform. Poly(*t*BuA) could not be dissolved. The spectra were measured at 298 K.

Polarizing Optical Microscopy (POM). Mesophases were identified with a Leica DMLD polarizing optical microscope equipped with a Linkam hot-stage. The thermotropic behavior of poly(EA) and poly(BnA) was studied between untreated glass slides using heating and cooling rates of 10 °C/min. The lyotropic behavior of the polymers was investigated using 20 wt % polymer solutions in CH_2Cl_2 at 25 °C.

Dynamic Mechanical Thermal Analysis (DMTA). Poly(EA) and poly(BnA) were tested on a PerkinElmer Diamond DMTA, using thin films with typical geometries: 15 × 5 x 0.05 mm. The films were cast from a CH_2Cl_2 solution using a doctor-blade on a Teflon substrate. The films were allowed to dry in air for 24 h. The poly(BnA) films were prepared by allowing the solvent to slowly evaporate. Fast evaporation resulted in highly crystalline films, which were brittle and difficult to handle. Subsequently both films were dried at 40 °C in an oven overnight under vacuum to remove any residual solvent and/or water. In the DMTA, the films were deformed in a cyclic sinusoidal mode with an amplitude of 2 μm and a static preload of 200 mN at four different frequencies, i.e., 0.1, 1, 10, and 100 Hz. All samples were heated from −100 to +175 °C using a heating rate of 2 °C/min under a nitrogen atmosphere.

Acknowledgment. This research was supported by The Netherlands Organisation for Scientific Research − Chemical Sciences (NWO−CW, VIDI project 700.55.426), the Dutch Polymer Institute (DPI projects nos. 622, 646, and 647), the European Research Council (ERC, EU seventh framework program, Grant Agreement 202886-CatCIR), and the University of Amsterdam.

Supporting Information Available: Figures showing chain growth−time profiles and IR and solid state NMR spectra of the (co)polymers. This material is available free of charge via the Internet at http://pubs.acs.org.

References and Notes

(1) Chen, E. Y.-X. *Chem. Rev*. **2009**, *109*, 5157–5214.
(2) (a) Collins, S.; Ward, D. G. *J. Am. Chem. Soc*. **1992**, *114*, 5460. (b) Bolig, A. D.; Chen, E. Y.-X. *J. Am. Chem. Soc*. **2001**, *123*, 7943. (c) Deng, H.; Shiono, T.; Soga, K. *Macromolecules* **1995**, *28*, 3067. (d) Cui, C.; Shafir, A.; Reeder, C. L.; Arnold, J. *Organometallics* **2003**, *22*, 3357.
(3) (a) Goode, W. E.; Owens, F. H.; Fellman, R. P.; Snyder, W. H.; Moore, J. E. *J. Polym. Sci*. **1960**, *46*, 317–331. (b) Hatada, K.; Kitayama, T.; Ute, K. *Prog. Polym. Sci*. **1988**, *13*, 189–276.
(4) For recent reviews on coordination-insertion copolymerization of polar monomers, see: (a) Boffa, L. S.; Novak, B. M. *Chem. Rev*. **2000**, *100*, 1479. (b) Ittel, S. D.; Johnson, L. K.; Brookhart, M. *Chem. Rev*. **2000**, *100*, 1169. (c) Nakamura, A.; Ito, S.; Nozaki, K. *Chem. Rev*. **2009**, *109*, 5215.
(5) Satoh, K.; Kamigaito, M. *Chem. Rev*. **2009**, *109*, 5120.
(6) For radical polymerization of dialkyl fumarates, see, for example: Toyoda, N.; Yoshida, M.; Otsu, T. *Polym. J*. (*Tokyo*) **1983**, *15*, 255.

(7) Jellema, E.; Jongerius, A. L.; Reek, J. N. H.; de Bruin, B. *Chem. Soc. Rev.* **2010**, *39*, 1706.
(8) (a) Ihara, E.; Fujioka, M.; Haida, N.; Itoh, T.; Inoue, K. *Macromolecules* **2005**, *38*, 2101–2108. (b) Ihara, E.; Kida, M.; Fujioka, M.; Haida, N.; Itoh, T.; Inoue, K. *J. Polym. Sci., Part A: Polym. Chem.* **2007**, *45*, 1536–1545. (c) Ihara, E.; Nakada, A.; Itoh, T.; Inoue, K. *Macromolecules* **2006**, *39*, 6440–6444. (d) Ihara, E.; Ishiguro, Y.; Yoshida, N.; Hiraren, T.; Itoh, T.; Inoue, K. *Macromolecules* **2009**, *42*, 8608–8610. (e) Ihara, E.; Hiraren, T.; Itoh, T.; Inoue, K. *J. Poly. Sci., Part A: Polym. Chem.* **2008**, *46*, 1638. (f) Ihara, E.; Hiraren, T.; Itoh, T.; Inoue, K. *Polym. J.* (*Tokyo*) **2008**, *40*, 1094. (g) Ihara, E.; Haida, N.; Iio, M.; Inoue, K. *Macromolecules* **2003**, *36*, 36.
(9) (a) Shea, K. J.; Walker, J. W.; Zhu, H.; Paz, M. M.; Greaves, J. *J. Am. Chem. Soc.* **1997**, *119*, 9049. (b) Busch, B. B.; Paz, M. M.; Shea, K. J.; Staiger, C. L.; Stoddard, J. M.; Walker, J. R.; Zhou, X.-Z.; Zhu, H. *J. Am. Chem. Soc.* **2002**, *124*, 3636. (c) Shea, K. J.; Busch, B. B.; Paz, M. M. *Angew. Chem., Int. Ed.* **1998**, *38*, 1391. (d) Wagner, C. E.; Kim, J.-S.; Shea, K. J. *J. Am. Chem. Soc.* **2003**, *125*, 12179. (e) Wagner, C. E.; Rodriguez, A. A.; Shea, K. J. *Macromolecules* **2005**, *38*, 7286.
(10) Hetterscheid, D. G. H.; Hendriksen, C.; Dzik, W. I.; Smits, J. M. M.; van Eck, E. R. H.; Rowan, A. E.; Busico, V.; Vacatello, M.; Van Axel Castelli, V.; Segre, A.; Jellema, E.; Bloemberg, T. G.; de Bruin, B. *J. Am. Chem. Soc.* **2006**, *128*, 9746–9752.
(11) Jellema, E.; Budzelaar, P. H. M.; Reek, J. N. H.; de Bruin, B. *J. Am. Chem. Soc.* **2007**, *129*, 11631–11641.
(12) Rubio, M.; Jellema, E.; Siegler, M. A.; Spek, A. L.; Reek, J. N. H.; de Bruin, B. *Dalton Trans.* **2009**, 8970.
(13) Jellema, E.; Jongerius, A. L.; Walters, A. J. C.; Smits, J. M. M.; Reek, J. N. H.; de Bruin, B. *Organometallics* **2010**, *29*, 2823–2826.
(14) For an overview of fully functionalized sp^2-hybridized polymers, polyisocyanides, see: Suginome, M.; Ito, Y. *Adv. Polym. Sci.* **2004**, *171*, 77.
(15) Patel, R. P.; Price, S. *J. Org. Chem.* **1965**, *30*, 3575–3576.
(16) Myhre, P. C.; Maxey, C. T.; Bebout, D. C.; Swedberg, S. H.; Petersen, B. L. *J. Org. Chem.* **1990**, *55*, 3417–3421.
(17) Otsu, T.; Yasuhara, T.; Shiraishi, K.; Mori, S. *Polym. Bull.* (*Heidelberg, Ger.*) **1984**, *12*, 449.
(18) Szwarc, M. *Nature* **1956**, *178*, 1168–1169.
(19) Beginn, U. *Colloid Polym. Sci.* **2008**, *286*, 1465–1474.
(20) Wang, L.; Broadbelt, L. J. *Macromolecules* **2009**, *42*, 7961–7968.
(21) Matyjaszewski, K.; Ziegler, M. J.; Arehart, S. V.; Greszta, D.; Pakula, T. *J. Phys. Org. Chem.* **2000**, *13*, 775–786.
(22) The small amount of homopoly(EA) was not observed in the GPC trace of the copolymer, probably due to the fact that the signals are overlapping and because the benzyl groups of BnA give rise to a much higher RI and UV response as compared to that of the EA components.
(23) Conversion of EDA with **1** after 30 min under the applied conditions: $\sim$ 70%; poly(EA) $M_w \sim$ 40 kDa.
(24) Reingruber, E. M.; Chojnacka, A.; Jellema, E.; de Bruin, B.; Buchberger, W.; Schoenmakers, P. J. Manuscript in preparation.
(25) Philipsen, H. J. A. *J. Chromatogr., A* **2004**, *1037*, 329–350.
(26) Chang, T. *Adv. Polym. Sci.* **2003**, *163*, 1–60.
(27) van Hulst, M.; Schoenmakers, P. *J. Chromatogr., A* **2006**, *1130*, 54–63.
(28) van der Horst, A.; Schoenmakers, P. J. *J. Chromatogr., A* **2003**, *1000*, 693–709.
(29) Ungar, G. *Macromolecules* **1986**, *19*, 1317.
(30) Li, L.; de Jeu, W. H. *Macromolecules* **2003**, *36*, 4862.
(31) Li, L.; de Jeu, W. H. *Phys. Rev. Lett.* **2004**, *92*, 075506/1–075506/3.
(32) Naga, N.; Yabe, T.; Sawaguchi, A.; Sone, M.; Noguchi, K.; Murase, S. *Macromolecules* **2008**, *41*, 7448.
(33) Ihara, E.; Goto, Y.; Itoh, T.; Inoue, K. *Polym. J.* (*Tokyo*) **2009**, *41*, 1117.
(34) Otsu, T.; Shiraishi, K.; Matsumoto, A. *J. Polym. Sci., Part A: Polym. Chem.* **1993**, *31*, 885.
(35) Mansur, C. R. E.; Tavares, M. I. B.; Monteiro, E. E. C. *J. Appl. Polym. Sci.* **2000**, *75*, 495.
(36) Otsu, T.; Yoshioka, M.; Matsumoto, A.; Shiraishi, K. *Polym. Bull.* (*Heidelberg, Ger.*) **1991**, *26*, 159.